B. KARPE, A. NAGODE, B. KOSEC, A. STOIĆ, M. DOLENEC, M. BIZJAK

ISSN 0543-5846
METABK 52(3) 305-308 (2013)
UDC – UDK 621.746:672:536.21=111

MICROSTRUCTURE EVOLUTION AND THERMAL STABILITY OF RAPIDLY SOLIDIFIED Al-Ni-Co-RE ALLOY

Received – Prispjelo: 2012-09-20
Accepted – Prihvaćeno: 2012-12-25
Original Scientific Paper – Izvorni znanstveni rad

In the frame of this work, Al-5Ni-1Co-3RE (RE-Rare Earth (Mischmetal)) rapidly solidified ribbons were manufactured and analyzed. The morphology of the as-cast structure, as well as the microstructural features were analyzed by transmission electron microscopy (TEM) and scanning electron microscopy (SEM). Thermal stability has been investigated by combination of four point scanning electrical resistivity measurement (ER), differential scanning calorimetry (DSC) and microhardness measurement. From the results we can conclude, that Al-5Ni-1Co-3RE rapidly solidified alloys have good thermal stability due to very slow coarsening kinetics of precipitated particles.

Key words: rapid solidification, metallic materials, heat transfer, precipitation, electrical resistivity measurement

INTRODUCTION

Aluminum alloys are commonly used as an engineering material for applications operating at lower temperatures [1,2]. For the synthesis of new aluminum alloys with good mechanical properties at elevated temperatures, a combination of powder metallurgy and rapid solidification is necessary. The largest hardening effect in Al based alloys is due to precipitation of extremely small, uniformly and densely dispersed particles in aluminum matrix [3]. Numerous studies have been carried out in this field. However, it is important to continually supplement our knowledge on the temperature stability of these types of materials.

The process of rapid solidification enables higher solubility of alloying elements in the α_{Al} solid solution. This is important in the production of alloys containing elements with low equilibrium solid solubility such as the transition group metals and lanthanides. In Table 1 maximal equilibrium solubility at room and eutectic/peritectic temperature for some low soluble alloying elements is presented [4].

Data concerning the extent and type of microstructural phases in microstructure of rapidly solidified aluminum alloys and their modifications during heating are important for controlling their properties. In the present work, the initial as-cast microstructure of the rapidly solidified Al-Ni-Co-RE alloy ribbons and the resulting microstructure after subsequent heat treatment as analyzed.

EXPERIMENTAL METHODS

An investigated aluminum alloy, with the chemical composition given in Table 2, was melted in inductive furnace in argon atmosphere and then rapidly solidified in a single roller melt spinning apparatus at various circumferential velocities.

For the microstructure characterization of the rapidly solidified ribbons, transmission electron microscopy (TEM), and scanning electron microscopy (SEM), were used. The sequence of microstructural changes during heating was recorded by measuring the electric resistance of the ribbons and scanning calorimetry (DSC). Samples for SEM observation were prepared according to classical metallographic procedure and etched with Keller's reagent. In order to observe the microstructure on surfaces parallel to the contact surface with the rotating wheel, the samples were ground down to defined thickness, polished and electrolytically etched. TEM observation samples were prepared by cutting out the disk-shaped specimens, which were then ion thinned and polished with Gatan PIPS M.691.

RESULTS AND DISCUSSION

All contemporary studies, concerning two or more component Al-TM rapidly solidified alloys, show different solidification morphologies across the transverse cross-section of the ribbon with clear dependence on the thickness of solidified ribbon [5,6]. Rapidly solidified Al-Ni-Co-RE alloy ribbons also show different morphologies across the ribbon thickness. Main reason for the distinctive layers (zones) is the direct connection between ribbon thickness and solidification velocity. At circumferential velocities of 35, 30 and 20 m/s, ribbon thicknesses between 15-25, 20-40, and 35-60 μm, were obtained. Rapidly solidified ribbons having thickness of up to 25 μm have a single featureless globular layer, which does not etch in Keller's reagent. Typical microstructure (Figure 1) of ribbons having a thickness be-

B. Karpe, A. Nagode, B. Kosec, M. Bizjak, Faculty of Natural Sciences and Engineering, University of Ljubljana, Ljubljana, Slovenia, A. Stoić, University of Applied Sciences, Slavonski Brod, Croatia.

Table 1 **Maximal equilibrium solubility at room and eutectic/peritectic temperature for some low soluble alloying elements [4]**

Element	Mass.%	T_e/T_p
Ni	0 ÷ 0,24	639,9
Co	≈ 0	657
La	0 ÷ 0,05	640
Ce	≈ 0	640
Pr	0 ÷ 0,05	640
Nd	0 ÷ 0,05	632
Fe	≈ 0	655
Zr	0 ÷ 0,16	660,8

Table 2 **Chemical composition of investigated alloy**

Element	Mass.%
Ni	4,6
Co	0,8
Re-Mish metal	3,0
Fe+Zr+Mn+Si	1,0
Al	Rest

tween 20-40 μm is composed of two layers. Globular layer at the contact surface with the rotating wheel (zone A) and cellular microstructure layer (zone B). Ribbons thicker than 45 μm have, along with zones A and B, high-temperature intermetallic phase particles visible on the free surface of the ribbon (zone C).

These particles can be seen in the center of columnar grains, as there grew radially outwards in a rosette like shape indicating that nucleation and growth started already in the melt. The morphology of ribbons having various thicknesses is shown in Figures l, Figure 3, Figure 4.

Zone A is composed of tiny globular grains. The presence of this zone is a consequence of a large undercooling, which occurs at the beginning of solidification through entire volume of the melt layer. Grains in this zone are between 2 and 5 μm in size, depending on the area being observed and the thickness of the ribbon.

Figure 2 represents calculated cooling curves in Al ribbon as a function of ribbon thickness and contact time with the cooling wheel [7], and Figure 3 cooling rate as a function of the ribbon thickness and distance from the wheel contact surface [8].

If the melt layer on the wheel surface is thin before the solidification is complete, the entire layer will be undercooled. This will result in a high solidification rate through the entire transverse cross-section of the ribbon. Because of the small volume of the melt and con-

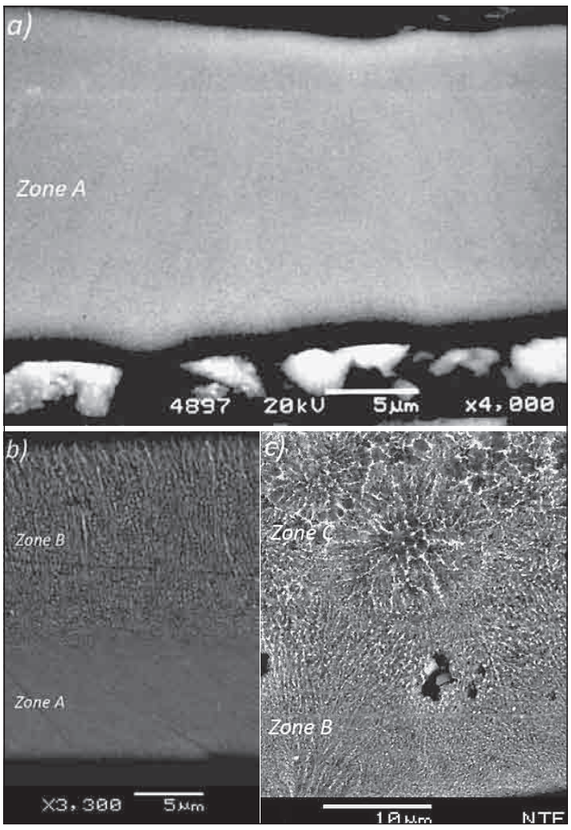

Figure 1 Morphologies of ribbons in a transverse cross-section: a) thickness 15 - 25 μm - rotation speed of 35 m/s, b) thickness 25-40 μm- rotation speed of 30 m/s, and c) thickness 35-60 μm - at a rotation speed of 20 m/s

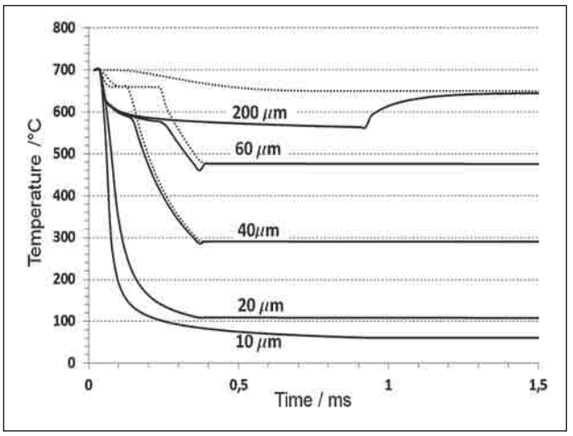

Figure 2 Al ribbon cooling curves as a function of its thickness [5]

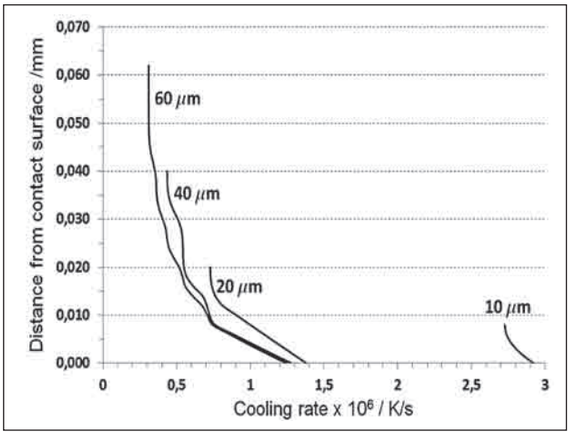

Figure 3 Cooling rate of Al ribbon as a function of its thickness and distance from the wheel contact surface [8]

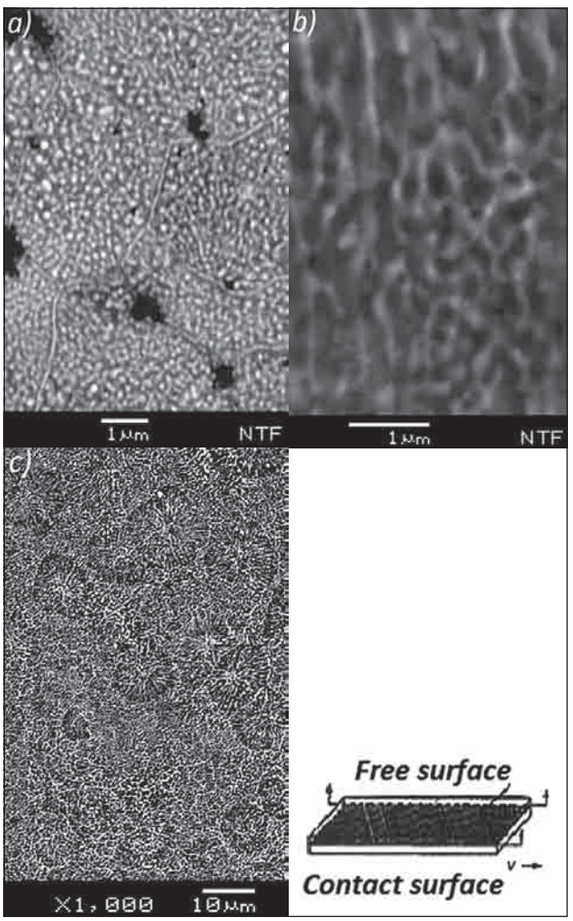

Figure 4 Morphology of ribbons having a thickness between 25-45 µm in a transverse cross-section: a) contact surface b) zone B and c) free surface (electrolytically etched - SEM)

sequently small amount of crystallization heat released, the cooling wheel is able to absorb all the crystallization heat [9]. This can be seen on the calculated cooling curve diagram (Figure 2) for the 10 and 20 µm thick ribbons as an absence of the temperature arrest of the free surface, contrary to thicker ribbons.

When the melt layer on the wheel surface is thicker, solidification at the contact surface starts before entire layer is undercooled. Some of the crystallization heat will be absorbed by the remaining melt, which will decrease its cooling rate and change the conditions for the nucleation. Furthermore, when a layer of defined thickness solidifies, thermal resistance in already solidified region of the melt layer becomes the limiting factor of the heat transfer, resulting in a decrease of the remaining melt cooling rate even further.

Uniform cooling and solidifying rates through entire cross section of the ribbon can be achieved only when very thin (< 25 µm) ribbons are cast (Figure 4). In this case zone B of the rapidly solidified ribbons has a cellular microstructure. Cell walls are composed of intermetalic phase particles. The cells in this zone are between 100 and 200 nm in size. In this core the zone C has rosette-like grains between 5 and 15 µm in size, and the grain boundaries contain even more intermetalic phase particles than those found in zone B (Figure 5). The center of those grains is composed of a supersaturated-solid solution α_{Al} as the primary phase, while the particles and cell walls form intermetalic phases rich in Al, Ni, Co and La. Intermetalic phase particles at the grain boundaries are richer in Ni, Co and La than the particles within the grains.

Figure 6 shows differential scanning calorimetry (DSC) curve and electrical resistance curve (ER) during heating at a constant rate of 5 K/min up to 600 °C.

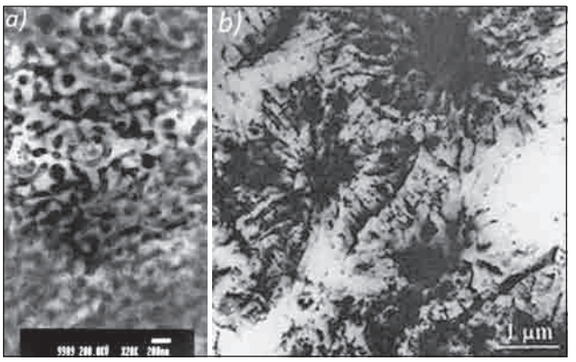

Figure 5 Microstructure of rapidly solidified Al-Ni-Co-RE alloy ribbons having a thickness greater than 45 µm: a) cellular micro structure- zone B (TEM) b) rosette like shape crystals on the free surface- zone C (TEM)

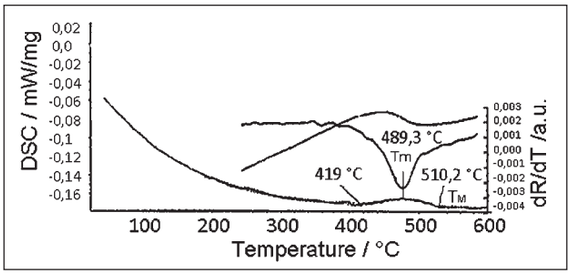

Figure 6 Comparison of the electrical resistivity and DSC curves as a function of temperature

Electrical resistivity increases linearly all the way up to 400°C and there is no exothermic peak on DSC curve. This means that heating the ribbons up to 400 °C does not affect their microstructure at all. At higher temperatures the change of electrical resistivity becomes nonlinear. At 489,3 °C it is evident, that an exothermic peak on the DSC corresponds to the minimum of the electric resistance first derivative temperature curve (dR/dT). During heating above the T_m or rather the T_M point, up to 510 °C, the cellular microstructure in zones B and C can still be observed. However, the transition to globular particles is also present. Larger differences can be observed on grain boundaries (Figure 7).

As the microstructure during heating changes, so does the microhardness. This is confirmed by microhardness measurements made on ribbons of various thicknesses after rapid solidification and thermal annealing up to 500 °C. An average value was calculated from a series of microhardness measurements. Influ-

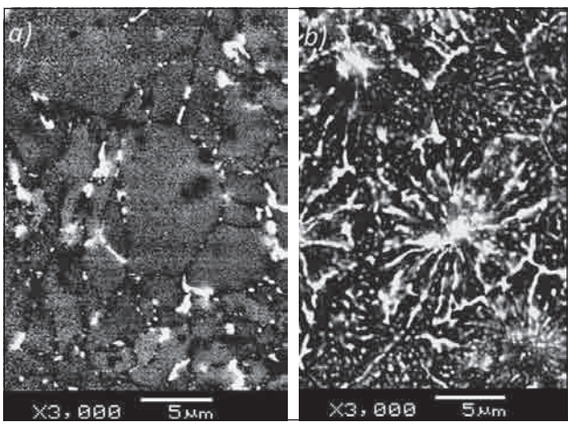

Figure 7 Microstructure of rapidly solidified Al-Ni-Co-RE alloy after heating at a constant rate of 5 K/min. up to 510 °C: a) zone B, b) zone C

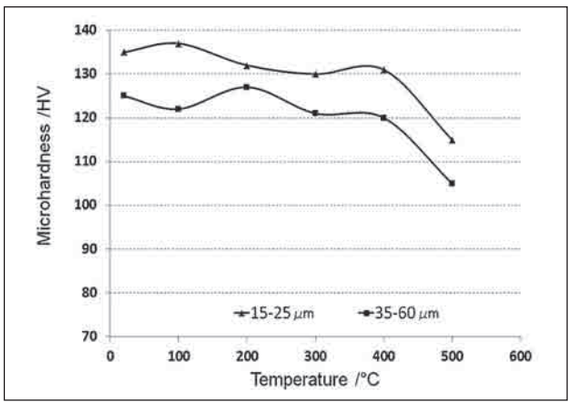

Figure 8 Vickers microhardness as a function of ribbon thickness and temperature

ence of temperature on the microhardness of ribbons having various thicknesses is presented in Figure 8.

Higher microhardness of thinner ribbons is a consequence of microstructure evolution and increased solubility of alloying elements in aluminum matrix α_{Al}.

The microhardness of rapidly solidified Al-Ni-Co-RE alloy ribbons remains nearly constant during heating at 5 K/min up to 400 °C. Decrease of the microhardness after heating above 400 °C indicates the precipitation of the alloying elements from the supersaturated α_{Al} solid solution in the form of fine intermetalic particles [10]. Temperature dependency of the microhardness is in good agreement with the electrical resistivity temperature dependency, which also shows nonlinear change above that temperature [11,12]. This can be seen more precisely on the first derivate electrical resistivity curve (dR/dT).

In comparison to the Al-Fe and Al-Fe-V alloys [12], the investigated Al-Ni-Co-RE alloy shows improved thermal stability in the temperature interval between 300 to 400 °C.

Shape of the fracture surface, with a distinctly pitted surface and a large number of deep oval concave pits, indicates that investigated alloy is extremely ductile and classifies it as a promising potential candidate for hot extrusion process.

CONCLUSIONS

The purpose of our investigation was to synthesize and investigate the temperature stability of aluminum alloy with addition of transition (Ni, Co) and lanthanide (RE-mischmetal) alloying elements beyond their maximum equilibrium solubility. We further wanted to confirm appropriate measurements for tracking the precipitation sequence from supersaturated solid solution α_{Al}.

From the results of our investigation can be concluded, that the rapid solidification by meltspinning technique enables higher solid solubility of added alloying elements in the aluminum matrix. The as-cast microstructure evolution is directly related to the thickness of the ribbon which governs the heat transfer and consequently nucleation event and solidification velocity. For higher supersaturation very thin (< 20 μm) ribbons need to be cast. Measurements of the electrical resistivity are closely linked to the microstructural changes in the rapidly solidified alloys and are in good agreement with differential scanning calorimetry (DSC) and microhardness measurements. The precipitation of intermetalic particles from supersaturated α_{Al} solid solution starts at temperature above 400 °C, when electrical resistivity becomes non-linear and last until 510 °C. The most intensive change in microstructure happened at ≈490 °C, where dR/dT minimum is detected. This is also in accordance with the exothermic peak on DCS curve and microhardness decrease at 500 °C.

REFERENCES

[1] H. H. Liebermann: Rapidly Solidified Alloys, Marcel Dekker, London, 1993.
[2] D. Klobčar, L. Kosec, A. Pietras, A. Smolej: Materials and Technology, 46(2012)5, 483-488.
[3] A. Inoue, H. Kimura: Solid State & Materials Science, 2(1997)3, 305-310.
[4] ASM International, Alloy Phase Diagrams Vol. 3, 1992.
[5] T. Haga, K. Inoue, H. Watani: Journal of Achievements in Materials and Manufacturing Engineering, 40(2010)2, 115-122.
[6] H. Jones: Journal of Materials Science, 19(1984)4, 1043-76.
[7] B. Karpe, B. Kosec, M. Bizjak, T. Kolenko: Metalurgija, 50(2011)1, 13-16.
[8] B. Karpe, M. Bizjak, B. Kosec: Journal of Achievements in Materials and Manufacturing Engineering, 46(2011)1, 88-94.
[9] G. X. Wang, E. F. Matthys: Modelling and Simulation in Material Science and Engineering, 10(2002), 35-55.
[10] J. Tušek, D. Klobčar: Journal of Mechanical Engineering, 50 (2004) 2, 94-103.
[11] I. Budak, M. Soković, M. Barišić: Measurement, 44 (2011) 6, 1188-1200.
[12] M. Bizjak, L. Kosec: Zeitschrift fuer Metallkunde, 91 (2000), 160-164.

Note: The responsible translator for English language is U. Letonja. MOAR, Podgora, Slovenia